Contribution from the School of Chemistry, University of Western Australia, Nedlands, Western Australia 6009, Australia, and The Rutherford Laboratory, Chilton, Didcot, Oxon OX11 OQX, England, U.K.

Spin Density of the Hexacyanochromate(III) Ion Measured by Polarized Neutron Diffraction

B. N. Figgis,*[1a] J. B. Forsyth,[1b] and P. A. Reynolds[1a]

Received April 22, 1986

A polarized neutron diffraction experiment on $Cs_2KCr(CN)_6$ yielded 437 unique magnetic structure factors, which were analyzed in terms of valence orbital or alternatively multipole populations on all atoms. Apart from a small population on the potassium atom, the spin density is described by a model corresponding to octahedral symmetry in the $Cr(CN)_6^{3-}$ ion with 3d and 4p orbitals on the chromium atom and $(sp)_\sigma$ and p_π orbitals on carbon and nitrogen atoms. The chromium configuration is $t_{2g}^{2.30(3)}e_g^{0.12(4)}4p^{0.83(7)}$ with the 3d orbitals expanded 8% radially relative to the free ion. The ligand atom σ and π orbital populations are $C_\sigma = -0.044$ (8), $C_\pi = -0.044$ (5), $N_\sigma = -0.034$ (7), and $N_\pi = 0.087$ (4). This complex spin density pattern is incompatible with molecular orbital theories of bonding that do not accommodate spin polarization effects, for example restricted Hartree–Fock. There is negative spin in the ligand σ framework and net positive spin in the π orbitals and in the metal 3d orbitals, with the $3d_\pi$ (t_{2g}) population less than the free-ion value of 3.00. These features are compatible with a model involving π back-bonding in the expected direction, which delocalizes spin from the t_{2g} to ligand π orbitals, together with spin polarization of about the same magnitude in the Cr–CN σ-bond. An approximate unrestricted calculation by the DV–Xα method shows fair agreement with our results, particularly in the cyanide ligand region. These results indicate that in this strongly covalent ion the electron–electron correlation effects on the *spin* distribution are of the same magnitude as the covalence effects.

Introduction

In the study of covalence and bonding in transition-metal complexes accurate measurement of charge and spin densities can provide unique information. This information, unlike most spectroscopic measurements, can be easily and directly related to the wave functions of theoretical calculations and provide a test of them. Relative to ionic values, the charge redistribution on bonding is small compared with the total number of electrons, which is usually dominated by the core. Even so, X-ray diffraction measurements are now sufficiently accurate to allow estimation of this redistribution with some reliability.

The spin distribution, because it involves only the highest lying molecular orbitals, is much more sensitive to bonding effects. The measurement of the spin density of a paramagnetic complex by the technique of polarized neutron diffraction (pnd) can provide a stringent test of theoretical wave functions. Measurement of *both* spin and charge density increases the constraints on the interpretation of bonding in the system.

Previous pnd measurements have largely involved either small symmetrical complexes, such as $CoCl_4^{2-}$,[2] $CoBr_4^{2-}$,[3] CrF_6^{3-},[4] or $FeCl_4^-$,[5] or larger less symmetrical molecules of more general chemical interest, for example the phthalocyanines of Co(II) and Mn(II)[6] or the $Fe(bpy)_2Cl_2^+$ cation.[5] The exception is the relative small and fairly covalent compound $Ni(NH_3)_4(NO_2)_2$,[7] which is, however, still too large and unsymmetrical to allow theoretical calculations of sufficient accuracy to fit the experimental results.[8] In these systems charge density results are available for $CoCl_4^{2-}$,[9] $Ni(NH_3)_4(NO_2)_2$[10] and $Fe(bpy)_2Cl_2^+FeCl_4^-$.[11]

The $M^{III}(CN)_6^{3-}$ ions are an obvious series in which an expectation of highly covalent bonding is combined with the requirements of smallness and high symmetry. Theoretical calculations on these ions are already available, the most recent examples being given in ref 12–14. Accordingly, we have commenced a study of the $Cr(CN)_6^{3-}$ ion. The charge densities in $[Co(NH_3)_5(H_2O)][Cr(CN)_6]$ and $[Co(NH_3)_6][Cr(CN)_6]$ have been analyzed,[15] and the analysis of $Cs_2KCr(CN)_6$ is in progress.[16] We present here a pnd study on $Cs_2KCr(CN)_6$, preliminary details of which have been reported already.[17]

The $Cr(CN)_6^{3-}$ ion has the orbitally nondegenerate ground term $^4A_{2g}$ ($S = {}^3/_2$), in which the spin is large enough for good accuracy in the pnd experiment. It also gives a negligibly small orbital magnetization correction to permit the extraction of the spin density from the experimental magnetization density data. A study of the $Fe(CN)_6^{3-}$ ion has also been undertaken[18] and a substantial amount of covalence is obviously present, but preliminary results indicate that there are complications due to the nature of the orbitally degenerate $^2T_{2g}$ ground term.

The general findings of previous experiments help to place this one in perspective.

(a) The major features of both spin and charge densities in all previous studies seem to be explained *qualitatively* by the wave functions of simple molecular orbital and other unsophisticated theories, including even ligand field theory.

(b) Current theoretical calculations underestimate the amount of covalence observed in small, simple, and rather ionically bound complex ions.

(c) A comparison of spin and charge densities suggests that electron correlation, viz. configurational interaction (CI), is important.

(d) Simple molecular orbital (MO) theories cannot quantitatively explain the charge *and* the spin densities in a complex ion *simultaneously*. That conclusion was already available from theoretical calculations of better type.

(e) The experiments are performed on *crystals*, and so a full comparison of theory and experiment should involve calculations that model the entire crystal. However, while longer range crystal effects are noticeable in the charge densities,[6,10,11,15] they seem much smaller in the spin densities. Distortions of ligand atoms

(1) (a) University of Western Australia. (b) The Rutherford Laboratory.
(2) Chandler, G. S.; Figgis, B. N.; Phillips, R. A.; Reynolds, P. A.; Williams, G. A. *Proc. R. Soc. London, A* **1982**, *384*, 31.
(3) Figgis, B. N.; Reynolds, P. A.; Mason, R. *Proc. R. Soc. London, A* **1982**, *384*, 49.
(4) Figgis, B. N.; Reynolds, P. A.; Williams, G. A. *J. Chem Soc., Dalton Trans.* **1980**, 2348.
(5) Figgis, B. N.; Reynolds, P. A.; Mason, R. *Inorg. Chem.* **1984**, *23*, 1149.
(6) (a) Williams, G. A.; Figgis, B. N.; Mason, R. *J. Chem. Soc., Dalton Trans.* **1981**, 734. (b) Figgis, B. N.; Williams, G. A.; Forsyth, J. B.; Mason, R. *J. Chem. Soc., Dalton Trans.* **1981**, 1837.
(7) Figgis, B. N.; Reynolds, P. A.; Mason, R. *J. Am. Chem. Soc.* **1983**, *105*, 440.
(8) Chandler, G. S.; Figgis, B. N.; Phillips, R. A.; Reynolds, P. A.; Mason, R. *J. Phys., Colloq.* **1982**, *No. 7*, 323.
(9) Figgis, B. N.; Reynolds, P. A.; White, A. H. *J. Chem. Soc., Dalton Trans.*, in press.
(10) Figgis, B. N.; Reynolds, P. A.; Wright, S. *J. Am. Chem. Soc.* **1983**, *105*, 434.
(11) Figgis, B. N.; Reynolds, P. A.; White, A. H. *Inorg. Chem* **1985**, *24*, 3762.
(12) Vanquickenborne, L. G.; Haspeslagh, L.; Hendrickx, M.; Verhulst, J. *Inorg. Chem.* **1984**, *23*, 1677.
(13) Sano, M.; Adachi, H.; Yamatera, H. *Bull. Chem. Soc. Jpn.* **1981**, *54*, 2898.
(14) Sano, M.; Kashiwagi, H.; Yamatera, H. *Inorg. Chem.* **1982**, *21*, 3837.
(15) Figgis, B. N.; Reynolds, P. A. *Inorg. Chem.* **1985**, *24*, 1864.
(16) Figgis, B. N.; Reynolds, P. A.; White, A. H. *J. Chem. Soc., Dalton Trans.*, in press.
(17) Figgis, B. N.; Forsyth, J. B.; Mason, R.; Reynolds, P. A. *Chem. Phys. Lett.* **1985**, *115*, 454.
(18) Brown, P. J.; Day, P.; Fischer, P.; Güdel, H. V.; Herren, F.; Ludi, A. *J. Phys., Colloq.* **1982**, *No. 7*, 235.

0020-1669/87/1326-0101$01.50/0

are particularly noticeable in the charge density maps. This may indicate that such effects are of relatively short range, so that the spin density, being metal-centered, is relatively more shielded than the charge density, where orbitals with large ligand coefficients are involved.

Experimental Section

Large amber single crystals of $Cs_2KCr(CN)_6$ were grown by slow cooling of a saturated solution of the ions in approximately the formula ratios. They belong to the monoclinic space group $P2_1/n$. The crystal structure has been determined by X-ray diffraction at 295 K[19] and neutron diffraction at 7.0 K;[20] a = 1.116 (1) nm, b = 0.829 (1) nm, c = 0.770 (1) nm, β = 90.3 (1)°, Z = 2, and T = 4.5 K.

A 51-mg crystal was mounted at 4.2 K on the D3 diffractometer of the Institut Laue Langevin, Grenoble, France, with b approximately parallel to the vertical axis, which is also the magnetic field direction. The imperfect alignment helps to minimize multiple-scattering effects. The magnetic field employed was 4.60 (1) T. The dimensions of the prismatic crystal were 6.0 × 3.0 × 1.2 mm ([100] × [101] × [001]). The polarization efficiency was 1.000 (1), the flipping efficiency was 1.000 (1), and the wavelength of the neutrons was 102.0 (1) pm. A total of 962 flipping ratios, $R(hkl)$, for 298 unique Bragg reflections of the form $\{hkl\}$, h = 0–4, were measured and the magnetic structure factors, $F_M(hkl)$, were derived by the use of the calculated nuclear structure factors, $F_N(hkl)$, by using the methods and corrections set out previously.[5] A second 48.5-mg crystal of similar habit was mounted with b approximately vertical and a further 1163 flipping ratios of the form $\{hkl\}$, l = 0–2, were measured for 310 unique reflections.

In the pnd experiment there is more uncertainty associated with reflections of very high or very low flipping ratio. Accordingly, all reflections with $R(hkl) > 2.0$ or <0.5 were rejected. Because of multiple scattering, the low values of $F_N(hkl)$ carry relatively large systematic errors, and so reflections for which $F_N(hkl) < 10^{-13}$ m were rejected also. The unpolarized neutron diffraction experiment on a similar crystal at 4.5 K required no extinction correction, and no evidence for extinction was present in the pnd data. As $R(hkl)$ is an intensity ratio, no correction for absorption was called for.

The two data sets were merged since in this material, at the temperature and magnetic field of the study, the magnetization should be isotropic, because of the simple ground-state term and very low ordering temperatures.

The ESR experimental g value of 1.99[2] is isotropic in the tripotassium salt. It was used in converting the magnetization density to the spin density. A magnetic moment of 2.50 (2) μ_B per chromium atom at the experimental magnetic field was established.[21]

The final 437 magnetic structure factors were produced after averaging equivalents measured on both crystals. The agreement factor between the equivalent reflections was $\sum(F_M(hkl) - \bar{F}_M(hkl))/\sum F_M(hkl) = 0.025$. $\sum\sigma(F_M(hkl))/\sum F_M(hkl)$ was 0.123. This relatively large value reflects the large number of reflections of relatively small F_M collected. These reflections with $h,+k,+l$ odd are weak in F_M since the Cr-centered spin contributes little to them. They thus serve to define ligand spin populations, and hence the covalence, much more precisely.

Fitting the Data

Although our data samples all regions of reciprocal space with (sin θ)/λ < 8 nm^{-1}, it is not complete within that region, because of limited experimental time and the rejection criteria. Direct Fourier transformation methods of analyzing the data are therefore not appropriate. Instead we perform least-squares fitting of an appropriate model for the spin density, ρ_s. We assume atom-centered distributions, ρ_i. T_i is the nuclear thermal motion observed for atom i in the neutron structure determination.[20]

$$\rho_s = \sum_i T_i C^i_{abc} R^a(K^i_a|r|)\, A^b_c(\theta,\phi)$$

$R^a|r|$ is a radial function, $A^b_c(\theta,\phi)$ an angular function, and C^i_{abc} and K^i_a are coefficients. An obvious and usual choice is to use theoretically calculated atomic radial functions for $R^a(|r|)$ and spherical harmonics $Y^b_c(\theta,\phi)$ for $A^b_c(\theta,\phi)$. Since the data are always limited and have associated errors, this series must be truncated. Our guide in such truncation is previous chemical knowledge and experience, and our test is the goodness-of-fit parameter, χ, which relates the parametrization of the model to the errors in the data. In this, as in other transition-metal complexes, we use for the radial functions those of the 3d and 4p orbitals calculated for an appropriate metal ion, here Cr^{2+}, $3d^34p^1$, and 2s and 2p functions on the carbon and nitrogen atoms. In other cases a pseudoatom (often H) centered midway between the metal atom and ligand donor atom to mimic overlap density has helped to improve the fit. Here we employ a Gaussian function of exponent 1.0 au^{-2}. The angular functions chosen may be all those spherical harmonics up to a certain order that are allowed by the crystallographic site symmetry, as in a "multipole analysis". However, as with the radial choice, these may be selected more efficiently by appeal to chemical knowledge. We can use a "valence orbital" parameterization in which only those multipoles involved in scattering from particular orbitals, or particular linear combinations of these (hybrid orbitals) are considered. For example scattering from 3d orbitals involves particular combinations of Y^0_0, Y^0_2, $Y^{\pm2}_2$, Y^0_4, Y^2_4, and $Y^{\pm4}_4$ but *not* of $Y^{\pm2}_3$ or Y^0_1. Such multipoles as $Y^{\pm2}_3$, which do not occur in simple LCAOMO theories of bonding, are found in multipole analyses to have much smaller coefficients than those of the allowed category. We note that such a valence orbital model can be generalized by the use of a sufficiently flexible basis set so that an infinite complete set is generated, which is equivalent to that of a full multipole analysis. One should also note that the valence orbital coefficients C^i_{abc} are *empirical parameters* and they only become true orbital populations if one assumes the validity of particular very simple theoretical models of bonding. Didactically such an assumption is often very illuminating, but for proper comparison with theory one should strictly use only the experimental spin or charge density and the wave functions of the calculations or some quantities rigorously derived from these.

Further constraints may be applied to the fitting process if appropriate local chemical rather than crystallographic symmetry is assumed. In our simplest refinement we assume octahedral symmetry for the $Cr(CN)_6^{3-}$ ion because the nuclear structure[20] very closely corresponds to that.

The parameters K^i_a are designed to accommodate empirically changes in the radial extent on incorporation of the "free ion" into bonding in the molecule. They are defined by the relationship $\langle j^i_n\rangle = \int r^2(R^i_a)^2 j^i_n(K^i_a\kappa r)\, dr$ where $j^i_n(\kappa)$ is the nth-order spherical Bessell function evaluated at wave vector κ, for the ith atom type. The $\langle j^i_n\rangle$ values occur as terms in calculating the structure factors.[10]

We employ the program ASRED.[10] Our most constrained refinement. R1, has 11 parameters. On Cr there are 3d-t_{2g} and 3d-e_g populations, with an associated radial parameter, K_{3d}, and a diffuse "4p" population. On each C and N atom there is a $2p_\pi$ and two sp hybrid orbital populations. $(sp)_1$ is directed toward Cr, and $(sp)_2$ is directed away from it. Lastly we have a mid-Cr–C-bond Gaussian population, p_{ov}, to model overlap spin density. The "4p" radius is more than twice as diffuse as that for 3d and this reduces correlation to acceptable levels.

In our more sophisticated model the refinement, R2, has fewer constraints. We abandon the constraints of octahedral symmetry so that C1–C3, N1–N3 and the Cr 3d and "4p" populations can vary independently. The number of parameters of this model rises to 32. The axis system chosen for Cr has z directed at C3 and x at C2.

Lastly, in refinement R3, we perform a partial multipole analysis. We retain the octahedral symmetry constraints on the multipoles belonging to the C and N atoms. On these we refine Y^0_0, Y^0_1, $^0_2$, and Y^0_3, thus retaining cylindrical symmetry in the cyanide group. On the major center of spin density, Cr, we employ all site-symmetry-allowed multipoles up to order 4, with the radial function chosen as that of the 3d orbitals, and a Y^0_0 term corresponding to "4p" orbitals in radius. In addition we refine density on the Cs and K sites: on Cs, Y, Y^0_1, $Y^{\pm1}_1$, Y^0_4, and $Y^{\pm4}_4$; on K, Y^0_0, Y^0_2, Y^0_4, and $Y^{\pm4}_4$. This latter set provides a test of whether spin transfer or polarization concerning the cations is appreciable. The model includes 34 parameters in all.

Results

The simple octahedral symmetry chemically based 11-parameter model, R1, gave R_w = 0.054 and χ = 1.386. The results are listed in Table I. A list of observed and calculated structure factors is available as supplementary material. All correlation coefficients were less than 0.82 in magnitude. Relaxation of the octahedral constraints to give the model corresponding to refinement R2 improves the fit somewhat: R_w = 0.046, χ = 1.198. The refined values of the parameters are set out in Table I. No individual parameters change relative to R1 at the 3σ confidence level. Refinement R3, the partial multipole analysis gave R_w = 0.045 and χ = 1.178. We do not list all the parameter values for this model since inspection shows the improvement relative to R1 is almost all in multipoles covered by refinement R2.

(19) Figgis, B. N.; Kucharski, E. S.; Reynolds, P. A.; White, A. H. *Acta Crystallogr., Sect. C: Cryst. Struct. Commun.* **1983**, *C39*, 1587.
(20) Brown, P. J.; Figgis, B. N.; Forsyth, J. B., submitted for publication in *Aust. J. Chem.* A total of 877 unique reflections collected to (sin σ)/λ = 7.3 nm^{-1} refined with anisotropic thermal parameters to R_w = 0.020.
(21) Forsyth, J. B., unpublished results.
(22) Baker, J. M.; Bleaney, B.; Bowers, K. D. *Proc. R. Soc. London, B* **1956**, *69*, 1205.

Table I. Results of the Octahedrally Constrained Valence Orbital Refinement (R1) and the Unconstrained Refinement (R2)[a]

atom		R1	R2			Xα calcn[26]
Cr	3d e_g	0.12 (4)	$d_{x^2-y^2}$ = 0.02 (2)	d_{z^2} = 0.14 (2)		0.30
	3d t_{2g}	2.30 (3)	d_{xy} = 0.76 (1)	d_{yz} = 0.76 (1)	d_{xz} = 0.75 (1)	2.62
	4p	0.83 (7)				0.12
K_{3d}		1.082 (4)	1.086 (4)			
			atom 1	atom 2	atom 3	
C	$(sp)_1$	−0.055 (6)	−0.049 (8)	−0.036 (8)	−0.080 (8)	−0.07
	$(sp)_2$	+0.012 (7)	+0.031 (10)	+0.004 (10)	−0.012 (10)	
	$2p_\pi$	−0.044 (5)	−0.052 (13)	−0.044 (13)	−0.026 (13)	−0.03
N	$(sp)_1$	−0.021 (5)	−0.041 (10)	−0.015 (10)	−0.003 (10)	0.00
	$(sp)_2$	−0.013 (3)	−0.014 (5)	−0.017 (5)	−0.005 (5)	
	$2p_\pi$	+0.087 (4)	+0.094 (5)	+0.096 (5)	+0.073 (5)	+0.09
	p_{ov}	−0.008 (7)	−0.006 (10)	−0.005 (10)	−0.013 (10)	

[a] All parameters except the radius K_{3d} are spin populations.

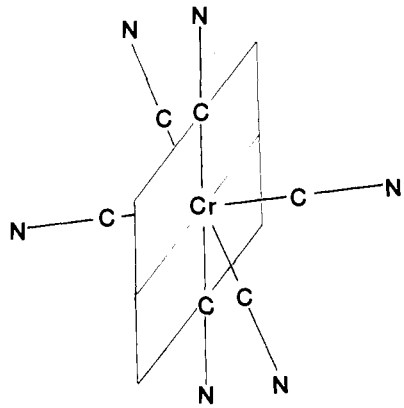

Figure 1. Plane for the spin density maps of Figures 2 and 3, containing two Cr–CN bonds (vertical) and bisecting the other Cr–CN axes.

Refinements R2 and R3 are essentially the same result cast in different forms. It is interesting to note that, apart from Y_2^{-1}, the multipoles exceeding the 3σ significance level are just those expected for 3d orbitals. In R3, as for R2, there is no strong evidence of nonoctahedral behavior. The population of multipoles of Cs and K are all found to be insignificant except for the spherical term on K. The total spin population on Cs is −0.002 (3), and on K it is 0.016 (5). In the refinements R1-R3 we can extrapolate the model to $(\sin\theta)/\lambda = 0$ to obtain the total magnetic moment for the two chromium atoms in the unit cell. The values are 4.98, 4.92, and 4.90 μ_B, respectively. Since these values agree well with the bulk magnetization measurement of 2.50 (2) μ_B per chromium atom, we are confident that we have accounted for all the spin in our modeling.

In charge density X-ray experiments it is usual to produce deformation density maps showing what part of the charge density on bonding is experimentally resolved. This operation performs a 2-fold function. First, a qualitative discussion of the changes is possible, and second, it suggests suitable functions that should be included in a model for least-squares fitting. In particular, it shows how the resolution limits the choice of such functions. As an extreme example, 4s and 4p atomic radial functions for transition metals differ in their model properties to only an experimentally unresolvable extent and are otherwise very similar. Thus, as in this case, we cannot refine simultaneously 4s and $4p_x$, $4p_y$, and $4p_z$ functions: we can only estimate the sum of 4s and 4p populations. That is why we have referred to "4p" populations.

In this, and in most other pnd experiments, the data are not complete, even within the $(\sin\sigma)/\lambda$ limit employed. Thus deformation spin density map construction by direct Fourier transformation of the experimental magnetic structure factors is not feasible, nor is the construction of a residual density map. However, to indicate the features resolved we *can* take the refined model, calculate a complete set of $F_M(hkl)$, within the $(\sin\theta)/\lambda$ limit, and perform the Fourier transformation. In Figure 1 we show the plane of the $Cr(CN)_6^{3-}$ ion in which the deformation density was evaluated by that procedure. The deformation density

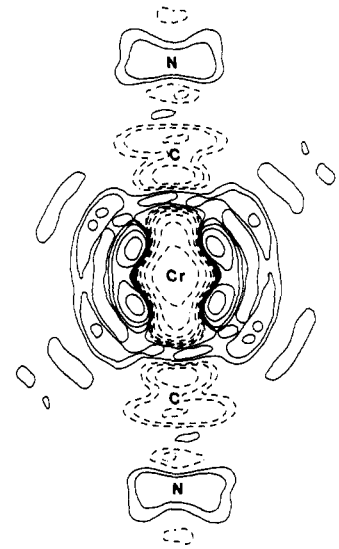

Figure 2. Dynamic deformation spin density in the plane specified by Figure 1 at the experimental resolution in the monoclinic crystal system. The Nth contour is at 10 N μ_B nm^{-3} with positive spin indicated by solid lines, negative spin by dotted ones.

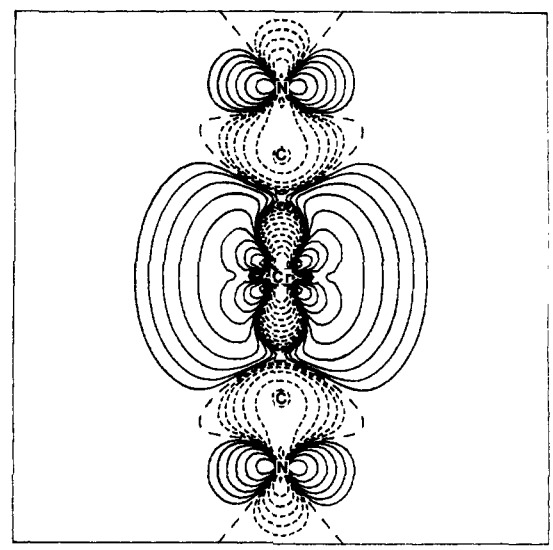

Figure 3. Model deformation spin density in the plane specified by Figure 1. The Nth contour is at $2^{(N-13)}$ spins au^{-3}.

is given in Figure 2. It can be seen that this figure does not quite retain the *mm* symmetry expected from an octahedral complex ion. That occurs because our procedure uses the monoclinic symmetry of the real crystal system. The deformation spin density is the observed model density minus that calculated for a spherically symmetrical Cr^{3+} ion from theory. The exact model

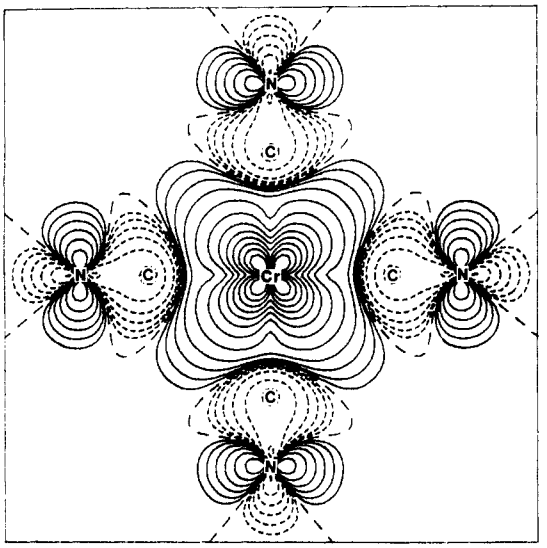

Figure 4. Total model spin density in a $Cr(CN)_4$ plane.

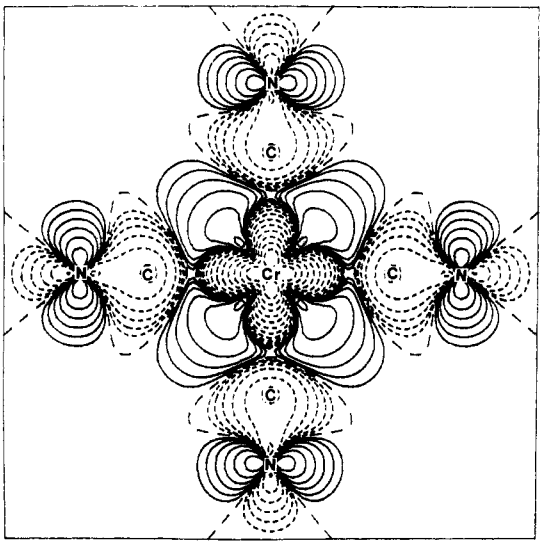

Figure 5. Model deformation spin density in the $Cr(CN)_4$ plane.

deformation spin density is shown in Figure 3. It was calculated from the orbital populations and radii of refinement R1 and the exact radial distributions by using the program MOPLOT. Figure 4 shows the model spin density in a plane containing four cyanide groups. Figure 5 is the corresponding *deformation* spin density, and Figure 6 is the *prepared-ion deformation* spin density, which we define as that of Figure 4 from which we have subtracted the spin density of a Cr^{3+} ion with a nonspherical $t_{2g}^3e_g^0$ configuration.

Qualitative Discussion

We shall discuss the qualitative features revealed by the modeling by reference to Figure 2. We observe substantial changes from a free Cr^{3+} ion in the spin density around the chromium atom. The spin distribution is changed in radial extent and is aspherical. The angular changes correspond to a preferred occupation of t_{2g} over e_g orbitals on the region of the 3d radius. This gives rise to a deficiency in the deformation density along the Cr–ligand axis and the peaks along the [111] cube axis (*xyz* direction). In our section this gives two holes vertically and four peaks at about 55° to the vertical. A simple electrostatic model of the bonding predicts the configuration $t_{2g}^3e_g^0$, and qualitatively that conforms with the figure. In addition such a model predicts an *expansion* of the t_{2g} radial wave function.[23] The spin deficiency near the chromium nucleus and the excess at greater distances conforms with such expansion.

(23) Craig, D. P.; Magnusson, E. A. *Discuss. Faraday Soc.* **1958**, *26*, 116.

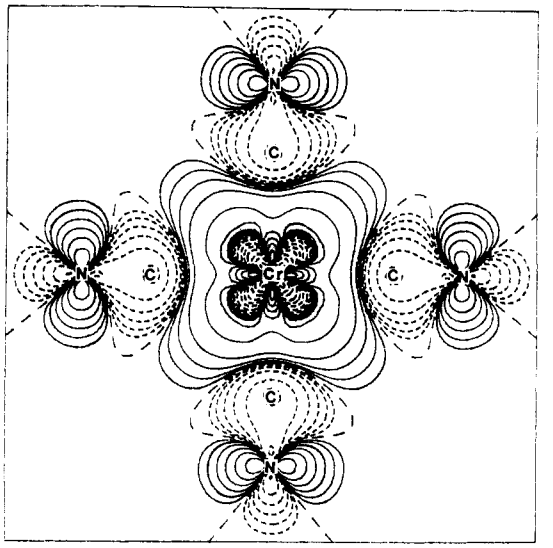

Figure 6. Model prepared-ion spin density in the $Cr(CN)_4$ plane, after subtraction of a $t_{2g}^3e_g^0$ theoretical Cr^{3+} ion spin density from the total model spin density.

This crystal field model predicts well the strongest features of the deformation density, which are around the chromium atom, but it does *not* predict any spin density on the cyanide ligand groups, such as is observed. The simplest model incorporating the covalence required to delocalize spin onto the ligands is a linear combination of atomic orbitals (LCAO) treatment for the molecular orbitals, in which *all* the spin is in a set of t_{2g} MO's

$$\Psi_{t_{2g}} = N_{t_{2g}}[|(Cr_{t_{2g}})\rangle + \lambda_\pi|(CN_{t_{2g}})\rangle],$$

where Ψ is the MO, N is the normalizing coefficient, and λ is the mixing coefficient between the chromium 3d and the ligand π orbitals. This constitutes the conventional "π-back-bonding" concept. We notice that the following features are predicted: (1) the spin is everywhere positive, (2) the spin occurs only in the π-system, and (3) there is a simple relation between the charge and spin densities in the π-system.

However, in the deformation density map we can see (1) significant negative spin, particularly on the carbon atom, and (2) negative spin in the σ system, along the Cr–CN axis, and on both carbon and nitrogen atoms, where the spin density is virtually identical. Although there is a large amount of positive spin of predominantly π-symmetry on the nitrogen atom, as the LCAO–MO model predicts, it is only comparable in magnitude with these unexplained features. We therefore conclude that the LCAO–MO model is inadequate and *that there is no simple relationship* between the spin and the charge densities, even at an approximate level, if covalence is included.

If we consider more sophisticated theoretical models that allow for electron correlation, on a qualitative level we have the prediction that the positive spin in the formally spin-paired σ-system will appear near the chromium atom, as spin polarization by a center attracts more like spin at the expense of creating opposite spin elsewhere. Consequently we expect the cyanide σ-system to be left with a net negative spin, as is observed.

We conclude then that if we look for an explanation of the experimental results at a level more detailed than that of crystal field theory and a $Cr(t_{2g}^3e_g^0)$ ion, we *must* consider electron correlation as well as relevant spin delocalization, since the effects are of comparable magnitude in the Cr–CN ligand bonding. Whereas the spin may be heavily polarized by the effects of electron correlation, the total charge density may be little affected by it. This makes calculation of charge densities easier, but it means they are unlikely to be as sensitive tests of bonding theories as are the spin densities.

Spin Density Maps. The spin density maps of Figures 3–6 are various representations of the fitted model density of refinement R1. The coefficients in the model are all well defined by the fitting process. We can see that, by comparison of Figures 2 and 3, which

show the same section. While Figure 3 appears much sharper, *no* extra density features have presented themselves. We should remember that the model has a number of theoretical approximations inherent, and, for example, the nodal behavior around the nitrogen atom should not be relied on in detail.

Figure 4 shows the model spin density in a $Cr(CN)_4$ plane. We note the concentration of spin on the chromium atom. It must be emphasized that the contours in these diagrams are in geometric progression. The density is negative on the ligand σ framework and positive in the nitrogen π orbitals. The spin density around the chromium atom is distinctly nonspherical. Figure 5 shows this more clearly since we have there subtracted a spherical Cr^{3+} ion density. It shows the large reduction in e_g and increase in t_{2g} spin densities. In addition, we can see, although less clearly, that the t_{2g} positive spin density appears to be expanded. Figure 6 shows this feature much more certainly. Here we have subtracted a cubic $t_{2g}^3e_g^0$ ion from the total spin density. The resultant remaining spin density can be thought of as representing the changes in spin density due to covalence, spin polarization, and intermolecular crystal field effects, if any, when a prepared octahedral "crystal field" Cr^{3+} ion bonds with the cyanide ligands. It therefore shows most clearly of all the diagrams the new features we have uncovered in this experiment. The ligand features are little changed from the previous maps. The chromium region shows that there is a positive 3d-e_g density, while close to the nucleus the t_{2g} orbitals have lost spin density. This is as expected from simple molecular orbital theories. However, at larger distances from the chromium atom there is a region of positive density, or mainly t_{2g} symmetry, which reflects 3d orbital radial expansion.

While these maps show such broad features unambiguously, there is a disquieting feature: in several places the difference spin density changes vary rapidly with distance. For example in the Cr–CN bond near the carbon atom. Such steep gradients are inherent with the simple theoretical models used for comparison with the data. More sophisticated models might avoid the high gradients but have not been developed in a form suitable for the present purposes. There is a need to use $Cr(CN)_6^{3-}$ molecular form factors in the initial fitting process.

Theory and the Observed Density. The $Cr(CN)_6^{3-}$ ion has been the object of several theoretical studies, the most recent of which are RHF calculations of good quality[12,14] and an unrestricted approximate calculation of the discrete variational Xα type[13] (DV–Xα).

RHF calculations are constrained to produce spin density that is everywhere positive. We observe significant negative spin density, for example a population of –0.088 (9) spins on the carbon atom. This is direct evidence of the inadequacy of such theories. It confirms the belief that such calculations are only qualitatively satisfactory for transition-metal complexes and that the road to improvement lies in the consideration of electron correlation effects and, possibly, of longer range "second-coordination-sphere" interactions. We can go further: RHF calculations are not even qualitatively correct for dealing with spin density results in more covalent systems; electron correlation *must* be included.

The inclusion of configurational interaction (CI), which is the form electron correlation takes, into Hartree–Fock calculations is a very large computational task for transition-metal complexes. Some calculations along these lines have been made, although not for the $Cr(CN)_6^{3-}$ ion. An alternative, less demanding approach, although much less sound theoretically, is to use an approximate calculation that includes electron correlation in some form. A calculation using the DV–Xα method is available for the $Cr(CN)_6^{3-}$ ion.[13] The agreement with our spin-density data is encouraging, being much improved over other calculations, as is seen by reference to Table I. In particular, we consider the ligand atom spin populations. The large negative spin in the carbon σ and π orbitals is duplicated, as are also the large positive nitrogen π-populations. The small nitrogen σ-population is calculated as zero. Thus the spin polarization on the cyanide ligands is predicted well by the calculation. If we turn to the metal atom we see that the positive population, arising from spin polarization of the σ orbitals is again reproduced, as is the reduction in the number of t_{2g} spins below 3.00, due to π-back-bonding. There are, however, some important quantitative differences between theory and experiment. Experimentally we obtain a reduction of 0.70 (3) spins in the t_{2g} orbitals, with a substantial, 8%, radial expansion of them, together with a large (0.83 (7) spins) diffuse metal–centered component. While here the difference from the DV–Xα calculation seems large, we must be careful not to attach too much significance to it at this stage. The DV–Xα calculation used a Mulliken population analysis to assign overlap contributions, while the experimental values are obtained by a least-squares population-fitting procedure. Consequently, rather different things are being compared. In addition, as Sano et al.[24] point out, in these hexacyano complex ions, as elsewhere, both charge and spin populations evaluated in the calculations are strongly basis-set dependent. Nevertheless, in examining the experimental spin density and UHF calculations for the $CoCl_4^{2-}$ ion in a more detailed and unbiased way,[2] we concluded that the comparison of numbers such as appear in Table I does allow an estimate of trends. Provisionally, we can suspect that the Xα calculation does not give a sufficient reduction in the t_{2g} orbtial occupation and underestimates the diffuse chromium centered orbital population. Whether this is a defect in the calculation or arises from the fact that the experimental data refers to a real crystal with intermolecular influences on the charge and spin densities, we cannot say. The charge density study of the $Cr(CN)_6^{3-}$ ion,[15] although on a different crystal system, involving the $[Co(NH_3)_5(H_2O)]^{3+}$ cation, also shows a distinctly smaller t_{2g} population than does the Xα calculation. Again, as for the spin density, the qualitative trends are correct. We defer further discussion of the charge density to a later paper in this series on the $Cr(CN)_6^{3-}$ ion.[16]

Acknowledgment. The authors are very grateful to the Institut Laue-Langevin for experimental time on the D3 diffractometer and to the Australian Research Grants Scheme for financial support.

Registry No. $Cr(CN)_6^{3-}$, 14875-14-0.

Supplementary Material Available: A list of anisotropic thermal parameters from the 7 K neutron structure refinement (1 page); a list of observed and magnetic calculated structure factors, with errors associated with the former, corresponding to refinement R1 (3 pages). Ordering information is given on any current masthead page.

(24) Sano, M.; Yamatera, H.; Hatano, Y. *Chem. Phys. Lett.* **1979**, *60*, 257.